Stanford Exploration Project, Report 114, October 14, 2003, pages 109–117

Short Note

Reflection tomography with depth control

Weitian Chen, Robert G. Clapp, and Biondo Biondi[1]

INTRODUCTION

Reflection tomography (Stork and Clayton, 1991; Stork, 1992; Clapp, 2001) is one of the most effective and widely used velocity estimation methods. However, reflection tomography has velocity-depth ambiguity problem (we do not know how much a traveltime error is due to a velocity error and how much is due to a reflector misposition) because of insufficient source-receiver offset and lateral velocity changes (Bickel, 1990; Lines, 1993; Ross, 1994; Tieman, 1994).

From borehole data, we can obtain the correct reflection positions around the borehole. The normal shift between the correct reflection positions and the apparent reflection positions can be linearly mapped to the traveltime perturbation along the normal ray (van Trier, 1990). However, from borehole data, we can only obtain the correct position for only a few reflection points along the borehole. In this paper, we assume all the reflection points within a local area around the borehole have the same normal shift. The normal ray traveltime perturbation for all these reflection points are then backpropagated simultaneously with the reflection traveltime perturbation. We applied this scheme on a synthetic model and obtained a better inversion result than using reflection tomography without this control. We further discuss how to improve this method for more complex datasets.

BASIC PRINCIPLES OF REFLECTION TOMOGRAPHY

For reflection data, there are two things that can cause traveltime perturbation: slowness perturbation Δs and reflector movement Δr. Figure 1 demonstrates the basic geometry for the reflection tomography problem. Here, l_n is the normal ray, l_o is the offset ray with aperture angle θ, and Δr is the normal shift between exact reflector and apparent reflector.

According to Fermat's principle, the traveltime perturbation caused by slowness perturbation, Δt_o, can be mapped approximately to slowness perturbation by the following linear

[1]**email:** chen@sep.stanford.edu, bob@sep.stanford.edu, biondo@sep.stanford.edu

relationship:

$$\Delta t_o \approx \int_{l_o} \Delta s dl_o. \tag{1}$$

According to van Trier (1990), the reflector movement Δr can be assumed equal to the residual zero-offset migration of the reflector. Consequently, Δr can be mapped to the slowness perturbation along the normal (zero-offset) ray, which can be expressed by the following equation

$$\Delta r \approx -\frac{1}{s_0} \int_{l_n} \Delta s dl_n, \tag{2}$$

where s_0 is the local slowness at the reflection point. According to Fermat's principle, the reflector movement Δr causes $-2\Delta r cos\theta$ change in ray length. As a result, the traveltime perturbation caused by reflector movement is

$$\Delta t_n \approx 2 s_o \Delta r cos\theta \approx -2 cos\theta \int_{l_n} \Delta s dl_n. \tag{3}$$

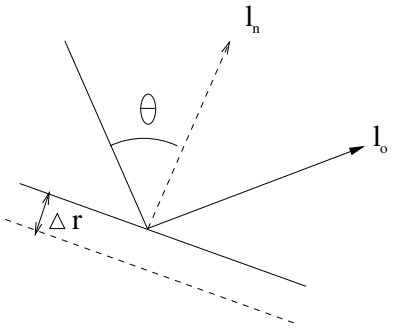

Figure 1: Geometry for reflection wave propagation. l_o is the offset ray. l_n is the normal ray. θ is the aperture angle of the offset ray. Δr is the normal shift between apparent reflector and correct reflector. chen1-ref [NR]

By summing Δt_o and Δt_n, we can obtain the total traveltime perturbation:

$$\Delta t = \Delta t_o + \Delta t_n \approx \int_{l_o} \Delta s dl_o - 2 cos\theta \int_{l_n} \Delta s dl_n. \tag{4}$$

Equation (4) provides a linear relationship between reflection traveltime perturbation Δt and slowness perturbation Δs which can be used for backpropagation.

For migration velocity analysis, reflection traveltime perturbation, Δt, can be effectively obtained from angle-domain common-image-gathers (ADCIG) (Clapp, 2001). Figure 2 is a sketch of ADCIG. Here, Δr is the normal shift between correct reflection position and apparent reflection position; Δr_2 is the residual moveout; and Δr_1 is the total normal shift. According to Biondi and Symes (2003), the traveltime perturbation Δt_o can be calculated from total normal shift by following equation:

$$\Delta t_o \approx 2 s_o cos\theta \Delta r_1. \tag{5}$$

Combining equation (5) and (3), we can obtain reflection traveltime perturbation from residual moveout by following equation:

$$\Delta t \approx 2 s_o cos\theta \Delta r_2. \tag{6}$$

As we can see, Δt_o and Δt_n can provide independent data information for velocity inversion. However, from reflection data, we can not obtain them separately since the reflection data alone can not provide the exact reflector position. Instead, we can only obtain Δt which is the sum of Δt_o and Δt_n for reflection tomography.

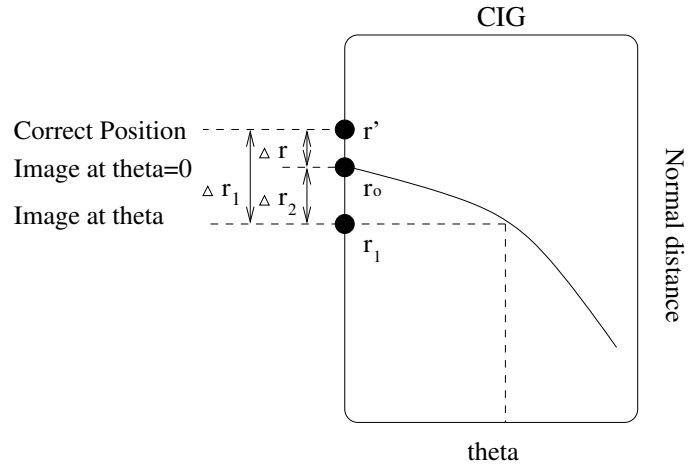

Figure 2: Illustration of calculating $\Delta\mathbf{t}$ for reflection tomography from angle-domain CIGs chen1-expl_data_adcig [NR]

DEPTH CONTROLLED REFLECTION TOMOGRAPHY

Borehole seismic data can provide the exact position of the subsurface reflectors at the borehole. Therefore, from borehole data, we can obtain Δr at these locations. Δr can be backpropagated to slowness perturbation using equation (2). In order to integrate the depth control to reflection tomography effectively, we transfer the reflector movement Δr to traveltime perturbation along normal ray, Δt_n. The traveltime perturbation Δt_n then is backpropagate to slowness perturbation using following equation:

$$\Delta t_n \approx -\int_{l_n} \Delta s dl_n \tag{7}$$

Combining equation (4) and (7), we can obtain a depth controlled reflection tomography (DCRT) scheme:

$$\Delta\mathbf{t} \approx \mathbf{T_r}\Delta\mathbf{s} \tag{8}$$

$$\Delta\mathbf{t_n} \approx \mathbf{T_n}\Delta\mathbf{s} \tag{9}$$

$$\mathbf{0} \approx \epsilon\mathbf{A}\Delta\mathbf{s} \tag{10}$$

Here, fitting goal (8) and (9) correspond to equation (4) and (7), respectively. Fitting goal 10 is the model styling goal. $\mathbf{A}$ is a regularization operator. We use a Laplacian as regularization operator for the following application.

RESULTS

We apply our DCRT scheme to a synthetic anticline model. Figure 3a and b show the correct velocity model and initial velocity model, respectively. There are seven reflectors for this synthetic model, which are overlayed on Figure 3b. A well is assumed at surface location $x = 10km$. Figure 4 shows the migration result using initial velocity model. The overlayed

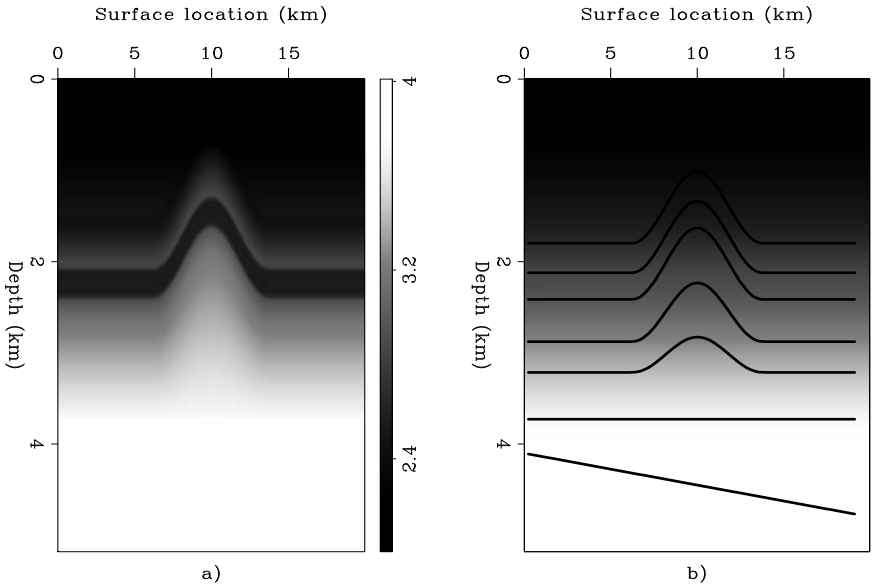

Figure 3: Synthetic anticline velocity model, a), and initial velocity model, b) chen1-vel [ER]

points are those reflection points we choose for backpropagation. For each reflector, we can only obtain the exact position for the reflection points where the well and the reflector cross. We make the assumption that all the reflection points within a local area around those reflection points have same normal shift. In Figure 5a, we show the assumed normal shift for all the reflection points we choose for adding depth control, which was used for DCRT in this application. As a comparison, in Figure 5b, we show the exact normal shift for those reflection points. After multiplying local slowness, we can obtain the corresponding traveltime perturbation along the normal ray. Figure 6a and b shows the assumed and exact normal ray traveltime perturbation, respectively.

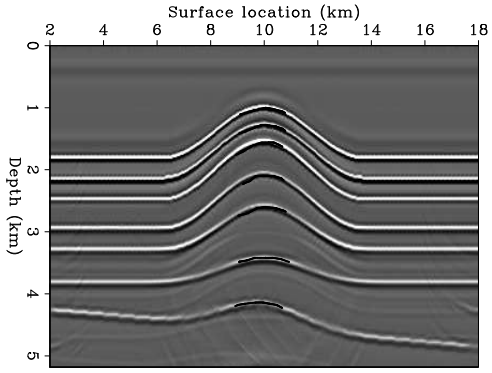

Figure 4: The migration result using initial velocity model. Overlayed are the reflection points chosen for adding depth points to reflection tomography chen1-crp [CR]

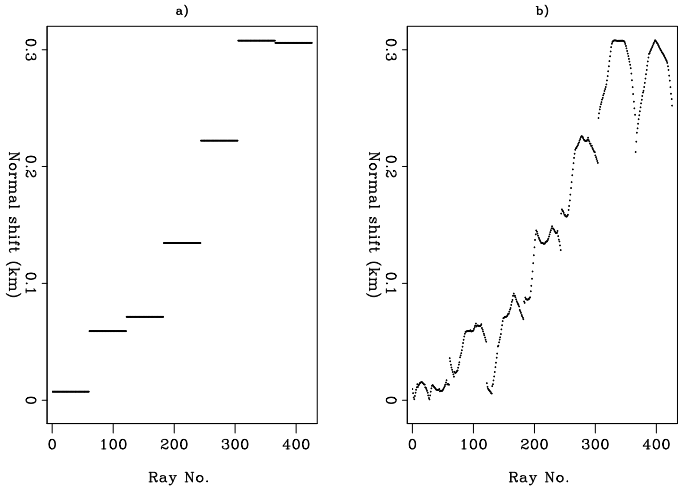

Figure 5: a) The approximated normal shift and b) the exact normal shift, for all the reflection points chosen for adding depth control. chen1-shift [ER]

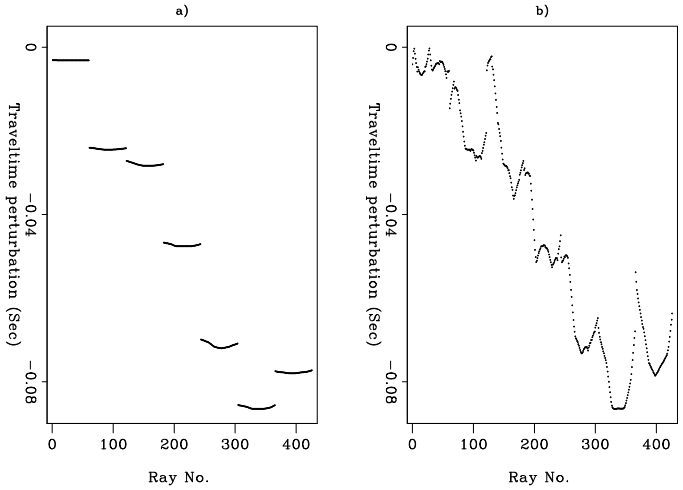

Figure 6: a) The approximated normal ray traveltime perturbation and b) the exact normal ray traveltime perturbation, for all the reflection points chosen for adding depth control chen1-travtime [ER]

The three panels in Figure 7, from left to right, show the inversion result of reflection tomography, DCRT, and their difference. Notice the obvious difference around the borehole between DCRT result and regular reflection tomography result. Figure 8 and Figure 9 shows the migration and angle-domain common-image-gathers (ADCIGs) using velocity obtained by regular reflection tomography and DCRT, respectively. The surface positions for 5 ADCIGs, from left to right, are 9.6, 9.8, 10, 10.2, 10.4 km, respectively. Notice the improvement of the image and the reduced residual moveout around the borehole after using the DCRT method.

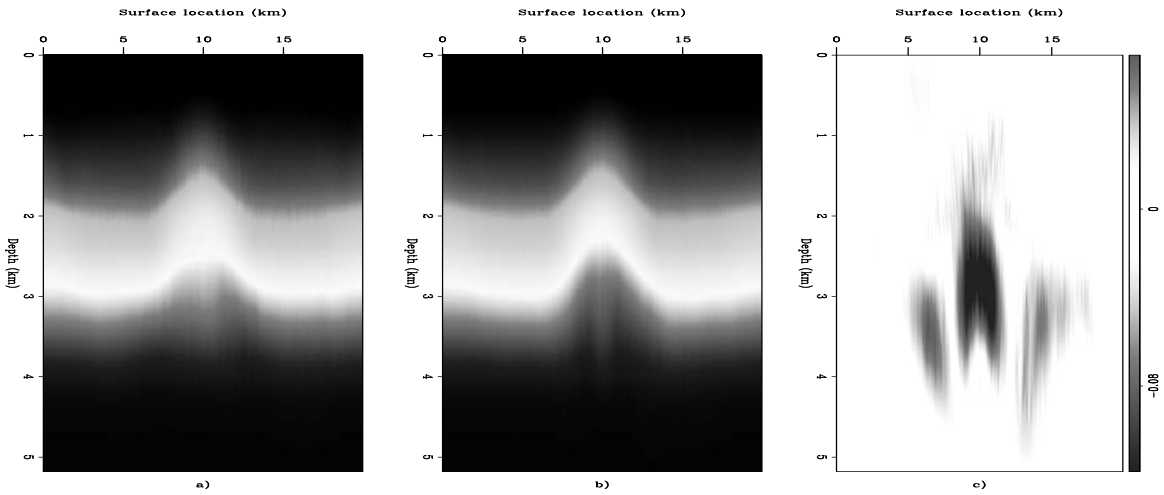

Figure 7: a) Reflection tomography result, b) DCRT result, and c) the difference between a) and b) chen1-allvel [ER]

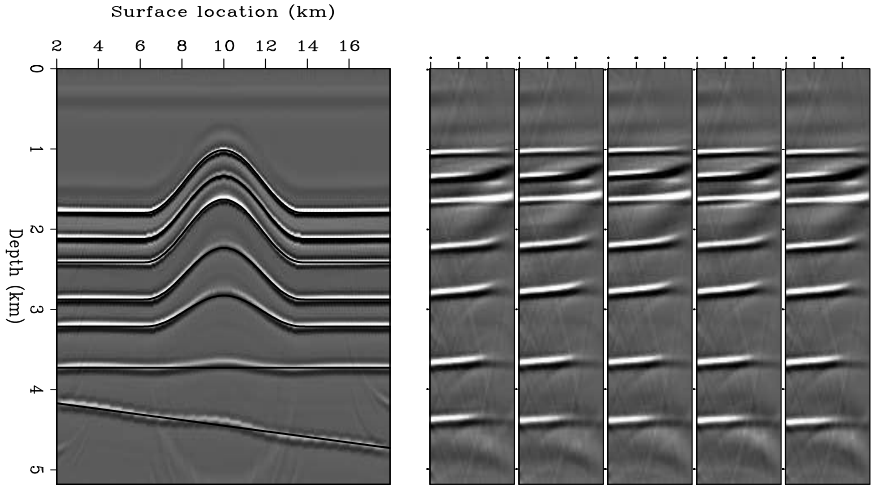

Figure 8: a) Migration result and b) ADCGIs, using velocity from reflection tomography. The surface location for 5 ADCIGs, from left to right, are 9.6, 9.8, 10, 10.2, 10.4 km, respectively. chen1-int.ref [CR]

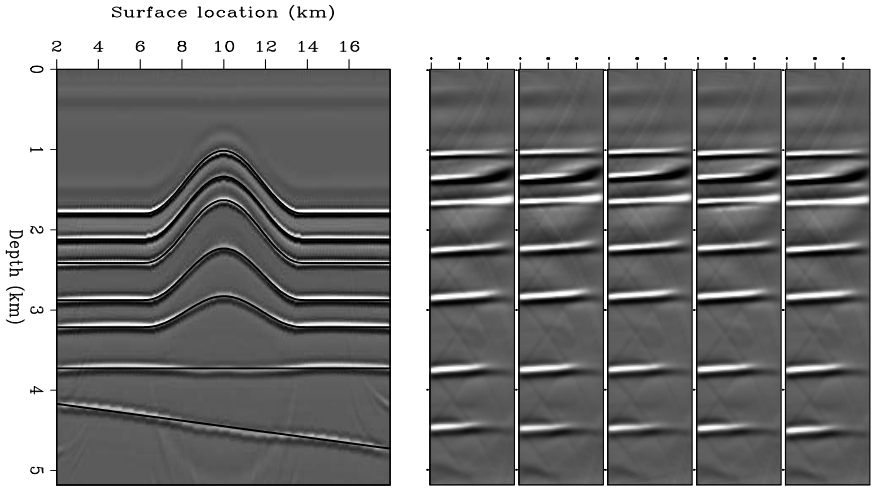

Figure 9: a) Migration result and b) ADCGIs, using velocity from DCRT. The surface location for 5 ADCIGs, from left to right, are 9.6, 9.8, 10, 10.2, 10.4 km, respectively. chen1-int.depth [CR]

DISCUSSION

In this shortnote, we presented a method to add depth control to reflection tomography. We transfer the exact reflector movement, which can be obtained from borehole data, to the traveltime perturbation along the normal ray. The traveltime perturbation along normal ray provides another data fitting goal for reflection tomography. By simultaneously backpropagating normal ray traveltime perturbation and reflection traveltime perturbation, we can improve the inversion result.

In the finished work, we obtained the normal shift between the correct reflection point and apparent reflection point, Δr, then transfer it to the traveltime perturbation along normal ray for backpropagation. Notice in Figure 2, by summing Δr and residual moveout Δr_2, we can obtain the total normal shift Δr_1, which can be transfered to traveltime perturbation along the offset ray according to equation (5). Therefore, instead of using equation (7) for backpropagation, we can backpropagate the traveltime along the offset ray by using the following linear relationship:

$$\Delta t_o = \int_{l_o} \Delta s dl_o. \tag{11}$$

An obvious advantage of backpropagating along the offset ray is that we can obtain better ray coverage. Backpropagating along normal ray can only obtain velocity along normal ray direction, whereas, when backpropagating along offset ray, we can obtain a much wider ray coverage with varying aperture angle of offset ray.

In the completed work, we did not apply any weighting between fitting goal (8) and (9). With an appropriate weighting scheme, the DCRT should improve the inversion result.

Another way to improve DCRT result is to use a spatially-varying Lagrange multiplier ϵ.

We assume all the reflection points within a local area have the same normal shift. Such an approximation is more reliable for the reflection points near the borehole, and less reliable for those points away from the borehole. In order to take this into account during inversion, we can apply spatially-varying ϵ to the model styling goal (10). We can apply small ϵ for the area close to the well to emphasize the data fitting, whereas big ϵ for the area away from the well to emphasize the model styling.

ACKNOWLEDGMENT

The first author would like to thank Stanford Graduate Fellowships for generously providing financial aids.

REFERENCES

Bickel, S. H., 1990, Velocity-depth ambiguity of reflection traveltimes: Geophysics, **55**, 266–276.

Biondi, B., and Symes, W., 2003, Angle-domain common-image gathers for migration velocity analysis: SEP–**113**.

Clapp, R., 2001, Geologically constrained migration velocity analysis: Ph.D. thesis, Stanford University.

Lines, L., 1993, Ambiguity in analysis of velocity and depth: Geophysics, **58**, 596–597.

Ross, W. S., 1994, The velocity-depth ambiguity in seismic traveltime data: Geophysics, **59**, 830–843.

Stork, C., and Clayton, R. W., 1991, Linear aspects of tomographic velocity analysis: Geophysics, **56**, 483–495.

Stork, C., 1992, Reflection tomography in the postmigrated domain: Geophysics, **57**, 680–692.

Tieman, H., 1994, Investigating the velocity-depth ambiguity of reflection traveltimes: Geophysics, **59**, 1763–1773.

van Trier, J. A., 1990, Tomographic determination of structural velocities from depth-migrated seismic data: Ph.D. thesis, Stanford University.